Available online at www.sciencedirect.com
ScienceDirect
Ceramics International 38 (2012) 211–216
CERAMICS INTERNATIONAL
www.elsevier.com/locate/ceramint

Determination of structural and mechanical properties of multilayer graphene added silicon nitride-based composites

Péter Kun, Orsolya Tapasztó, Ferenc Wéber, Csaba Balázsi *

Ceramics and Nanocomposites Department, Research Institute for Technical Physics and Materials Science, Konkoly-Thege ut 29-33, H-1121 Budapest, Hungary

Received 15 June 2011; received in revised form 24 June 2011; accepted 25 June 2011
Available online 2nd July 2011

Abstract

Silicon nitride based nanocomposites have been prepared with different amount (1 and 3 wt%) of multilayer graphene (MLG) as well as exfoliated graphite nanoplatelets (xGnP) and nano graphene platelets (Angstron) in comparison. The microstructure and mechanical properties of the graphene reinforced silicon nitride based composite materials have been investigated. Homogeneous distribution of the MLG additives have been observed on the fracture surface of the sintered material. The scanning electron microscopy examinations showed that graphene platelets are inducing porosity in matrix. The bending strength and elastic modulus of MLG/Si_3N_4 composites showed enhanced values compared to the other graphene added silicon nitride ceramic composites. These observations may be explained by the different type and quality of the starting materials and by the dispersion grade of graphene platelets having direct impact to the resulting density of the sintered samples.

Keywords: B. X-ray methods; C. Mechanical properties; D. Si_3N_4; Graphene; Scanning electron microscopy

1. Introduction

Although diamond and graphite have been well known for centuries, nanosized allotropes of carbon such as fullerenes, nanotubes and lastly graphene have been only discovered in our time. The monolayer graphene is one atom thick sheet composed of hexagonal structure of carbon atoms, however graphene samples with two or more layers are being investigated with equal interest. This two dimensional material has been characterised by exceptional electrical, mechanical and thermal properties [1–5]. It had been turned out that electrons to move ballistically in graphene layers with a mobility which can be exceed 200,000 $cm^2\ V^{-1}\ s^{-1}$. Beside that the graphene were found to have unique thermal conductivity: even 5300 W/mK. In addition it has superior mechanical properties with Young's modulus of approximately 0.5–1.0 TPa. Interestingly, despite of their non-perfect structure, even suspended graphene oxide sheets retained almost a Young's modulus of 0.25 TPa. These values indicate that graphene can be applied as an excellent reinforcement to ceramic materials.

Therefore, it is expected that the addition of graphene-based materials will significantly improve the properties of different matrices, such as polymer, metal and ceramic. There has been significant effort to use graphene in polymer composites. Ramanathan et al. [6] reported that functionalized graphene sheets are well suited to form composites with polymers such as PMMA, PAN and PAA. This nanofiller offers properties that are equal to or better than those of singlewall carbon nanotubes (SWCNTs). Although there are only few reports on the use of graphene in ceramics, recently Fan et al. [7] have prepared graphene nanosheets reinforced alumina matrix composites. The electrical conductivity of that composite outperformes the conductivity of the carbon nanotube/Al_2O_3 composites.

The research of ceramic composites incorporated with carbon-based fillers has focused on carbon nanotubes (CNTs) until now. In the last decade various CNT-reinforced ceramic systems have been developed and improved properties of these composite materials have been reported in a number of works. Carbon nanotubes–metal–ceramic nanocomposites (metal: Fe, Co, Ni; ceramic: Al_2O_3, $MgAl_2O_4$ and MgO) have been prepared by hot pressing by Peigney et al. [8]. In that work the nanotube bundles grown in situ, however it had not caused significant improvement in mechanical properties. Only modest improvements of mechanical properties were reported in CNTs

* Corresponding author. Tel.: +36 1 392 2249; fax: +36 1 392 2226.
E-mail address: balazsi@mfa.kfki.hu (C. Balázsi).

0272-8842/$36.00
doi:10.1016/j.ceramint.2011.06.051

reinforced silicon carbide [9] and silicon nitride matrix composites [10,11]. However significant increase in bending strength and fracture toughness has been achieved in CNTs reinforced alumina matrix composites [12–15]. In contrast to this another research group have not found increments in toughness, but significantly improved contact-damage for these composites [16]. Considerable high increase of electrical conductivity has been achieved in carbon nanofibers-zirconia composites [17] and CNTs reinforced silicon nitride matrix composites [10,18–20]. Beside that it was found that carbon nanotubes can lower the thermal conductivity [21] and the friction coefficient [22] in silicon nitride composites. Very soon it turned out that the main difficulty in composite preparation seems to be the achievement of the suitably homogenous dispersion of CNTs in the matrices because this material have preference for agglomeration in a matrix. Moreover, it is also important to achive a good densification of the components and to avoid the high degradation of the nanofillers. It can be mentioned that colloidal processing can help the formation of highly dispersed CNTs/ceramic composites as it was found in alumina [23] and silicon nitride-based [24] matrices.

In this work multilayer graphene reinforced silicon nitride-based ceramic composites by a two-step sinter-HIP method have been prepared. The use of the optimal temperature and pressure, holding time helped to avoid the notable damaging of graphene during high temperature processing thus the graphene have been preserved in composites. Beside that the effective dispersion of graphene-based materials in the matrix has been achieved. The microstructure and mechanical properties of the graphene reinforced ceramic composite materials are presented.

2. Experimental

The starting materials used in experiments were as follows: 90 wt% Si_3N_4 (Ube, SN-ESP), as well 4 wt% Al_2O_3 (Alcoa, A16) and 6 wt% Y_2O_3 (H.C. Starck, grade C) to aid the sintering process. Polyethylenglycol (PEG) surfactants and deionized water were added to the powder mixture. These mixtures were milled in high efficient attritor mill (Union Process, type 01-HD/HDDM) equipped with zirconia agitator delta discs (volume of 1400 cm^3) and zirconia grinding media (diameter of 1 mm) in a 750 ml silicon nitride tank. Each batch contained zirconia as contamination from media and discs. This milling process has been performed whith high rotation speed, 3000 rpm until 4.5 h.

Different type of multilayer or few-layer graphene were used as reinforcement material for ceramic matrices. In this current work multilayer graphene nanosheets were prepared by mechanical milling method [25] similar to method used by Knieke et al. [26]. For many applications this process can be a simple and efficient way for graphene production. In brief commercial graphite powder (Aldrich) has been milled intensively in high efficient attritor mill in presence of ethanol until 10 h. As comparision another graphene-based materials were included to this study: exfoliated graphite nanoplatelets (xGnP-M-5 and xGnP-M-25) [27,28], and nano graphene platelets (Angstron N006-010-P) [29]. The scanning electron micrographs of these graphene-based materials can be seen in Fig. 1. Thus 1 or 3 wt% of graphene nanoplatelets were mixed with the silicon nitride-based powder mixture in attrition mill with low rotational speed, 600 rpm until 30 min. Starting compositions of sintered samples can be found in Table 1.

The substance was dried and sieved with a filter with mesh size of 150 μm. Green samples were obtained by dry pressing at 220 MPa. Samples prepared for HIP were oxidized at 400 °C to eliminate the PEG. Hot isostatic pressing (HIP) was performed at 1700 °C in high purity nitrogen by a two-step sinter-HIP method using BN embedding powder at 20 MPa, with 3 h holding time. The heating rate did not exceed 25 °C/min. The dimensions of the as-sintered specimens were 3.5 mm × 5 mm × 50 mm.

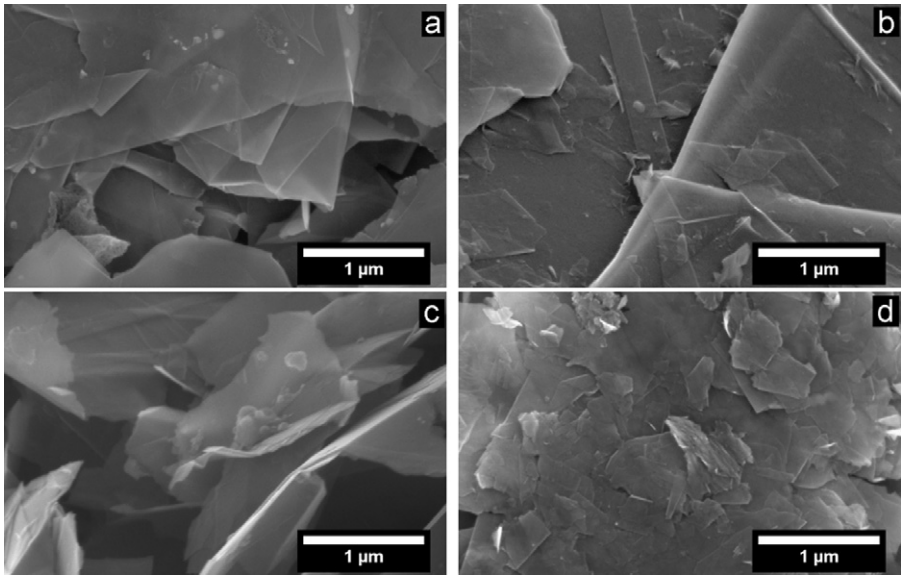

Fig. 1. Scanning electron micrographs of the starting graphene materials: a) xGnP-M-5, b) xGnP-M-25, c) Angstron N006-010-P, d) multilayer graphene (MLG).

Table 1
Starting compositions of sintered samples.

Batch	Starting powders (wt%)			Carbon (wt%)	Type of additives	Milling (in water)	Mixing (in water)	Sintering conditions		
	Si_3N_4	Al_2O_3	Y_2O_3			3000 rpm	600 rpm	Temperature (°C)	Holding time	Pressure (MPa)
HIP1	90	4	6	1	xGnP-M-5	4.5 h	0.5 h	1700	3 h	20
HIP2	90	4	6	1	xGnP-M-25	4.5 h	0.5 h	1700	3 h	20
HIP3	90	4	6	1	Angstron N006-010-P	4.5 h	0.5 h	1700	3 h	20
HIP4	90	4	6	1	Multilayer graphene	4.5 h	0.5 h	1700	3 h	20
HIP5	90	4	6	3	xGnP-M-5	4.5 h	0.5 h	1700	3 h	20
HIP6	90	4	6	3	xGnP-M-25	4.5 h	0.5 h	1700	3 h	20
HIP7	90	4	6	3	Angstron N006-010-P	4.5 h	0.5 h	1700	3 h	20
HIP8	90	4	6	3	Multilayer graphene	4.5 h	0.5 h	1700	3 h	20

After sintering the weight change of the samples was precisely determined. The density of the sintered materials were measured by Archimedes method. Morphology and microstructure of the materials were studied by scanning electron microscope, (SEM, Zeiss-SMT LEO 1540 XB). Phase compositions were determined by X-ray diffractometer (Bruker AXS D8). The elastic modulus and the four-point bending strength values for HIP samples were determined by bending tests on a tensile/loading machine (INSTRON-1112).

3. Results and discussions

The characteristic morphologies of the 1 wt% MLG (multilayer graphene) added silicon nitride composite can be seen in Fig. 2. On the fracture surface of the sintered material the homogeneous distribution of the MLG additives can be observed in Fig. 2a as it is showed by arrows. In Fig. 2a porosities can be also observed. In Fig. 2b a well embedded MLG layer into silicon nitride matrix is presented. This particular MLG has 0.3–0.4 μm in length and thickness of approximately 10 nm. In the work made by Fan et al. [7] the most pulled-out sheets are ~50 nm thick. They mentioned that it is difficult to find thin sheets (below 20 nm) on the fracture surfaces because there are hard to identify in a SEM micrograph.

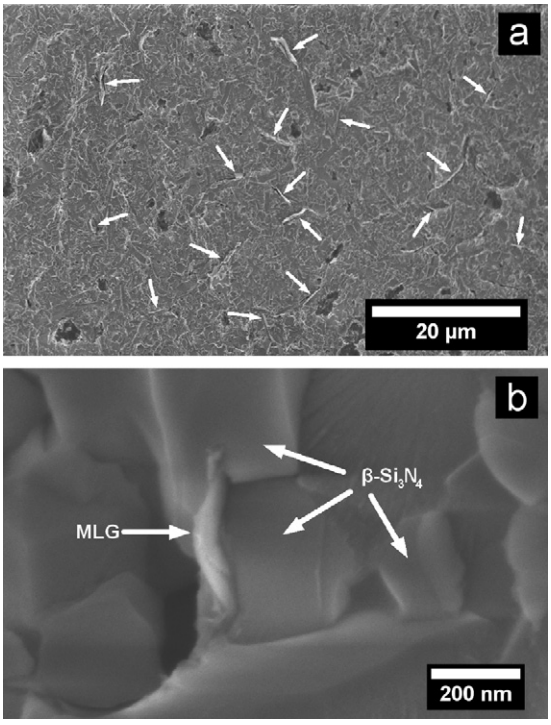

Fig. 2. Fracture surfaces of HIP4 (1 wt% multilayer graphene (MLG) added Si_3N_4) a) homogen dispersion of MLG showed by arrows, b) MLG connected silicon nitride.

The scanning electron micrographs of the fracture surfaces of the different type of 1 wt% graphene additions (Fig. 3a: HIP1, Fig. 3b: HIP2, Fig. 3c: HIP3, Fig. 3d: HIP4) can be seen on Fig. 3. In these micrographs not only the distribution, but the local contacts between the matrix and the graphene additions can be observed. The location of embedded graphene are shown by white arrows. It can be seen that in all of the cases good distribution is achieved. It can be observed that graphene platelets are inducing porosity in matrix (Fig. 3a and d). This may cause the deteriation of mechanical properties. A possible solution for this problem would be using smaller starting graphene nanoplatelets and improving the further separation of aggregates or prevent the agglomeration of graphene platelets during the fabrication processes.

In Fig. 4 the fracture surfaces with different type of 3 wt% graphene additions (Fig. 4a: HIP5, Fig. 4b: HIP6, Fig. 4c: HIP7, Fig. 4d: HIP8) can be seen. The local environment of the distributed graphene nanoplatelets are shown by white arrows. In these cases similar morphologies to 1 wt% graphene additions may be observed. There are some pronounced presence of induced porosity by graphene addition. Huge β-Si_3N_4 grains that are usually developing through gase-phase processes [30] in addition to liquid phase sintering can be found on Fig. 4b.

The microstructural investigation by the help of X-ray diffraction of the sintered samples are presented in Fig. 5 and Fig. 6. In the X-ray micrographs the characteristic patterns in the case of 1 wt% (Fig. 5) and 3 wt% (Fig. 6) graphene content with different type of additions can be observed. The diffraction peaks of β-Si_3N_4 (JCPDS-PDF 33-1160) and $ZrO_{1.96}$ (JCPDS-PDF 81-1546) can be recognized in all cases. The results showed that the graphene added silicon nitride composite has

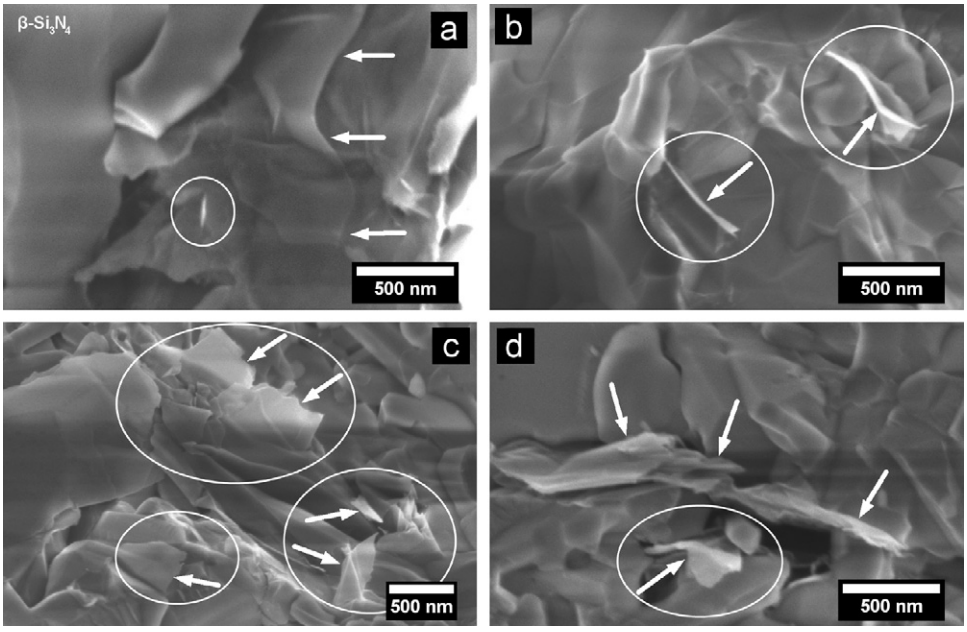

Fig. 3. Fracture surfaces of the sintered samples (1 wt% graphene added): a) HIP1, b) HIP2, c) HIP3, d) HIP4.

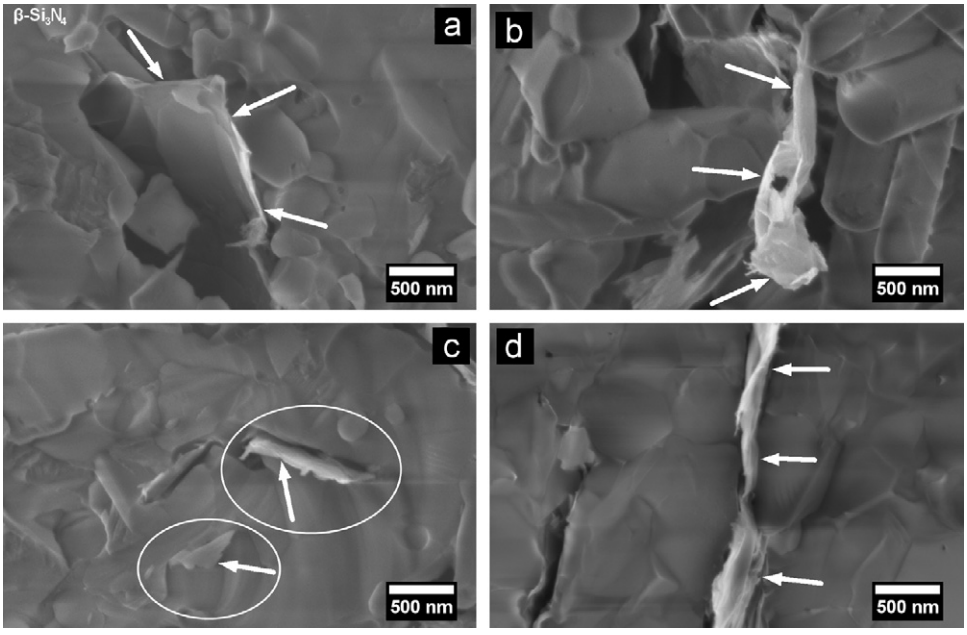

Fig. 4. Fracture surfaces of the sintered samples (3 wt% graphene added): a) HIP5, b) HIP6, c) HIP7, d) HIP8.

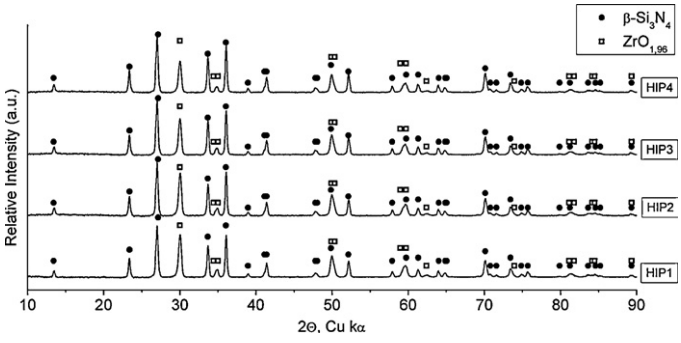

Fig. 5. XRD patterns of the sintered silicon nitride-based composites with 1 wt% graphene addition.

only β-Si_3N_4 phase, the α → β-Si_3N_4 transformation is completed. The main line of the graphite (JCPDS-PDF 12-0212) only in the case of 3 wt% carbon contents at $2\theta = 26.44^\circ$ ($d = 0.337$ nm using Bragg's law ($n\lambda = 2d\sin(\theta)$) can be observed. This graphite peak is more pronounced in the case of HIP7 and HIP8. In the case of HIP8 a new phase appeared with low intensity peaks. The main lines of Si_2N_2O (JCPDS-PDF 18-1171) (Fig. 6) at $d = 0.468$ nm, $d = 0.444$ nm, $d = 0.273$ nm, $d = 0.242$ nm can be observed.

The mechanical properties (modulus of elasticity and bending strength) of the sintered samples are shown in Figs. 7 and 8. A summary of measurement data can be seen in Table 2. The average modulus of elisticity can be observed

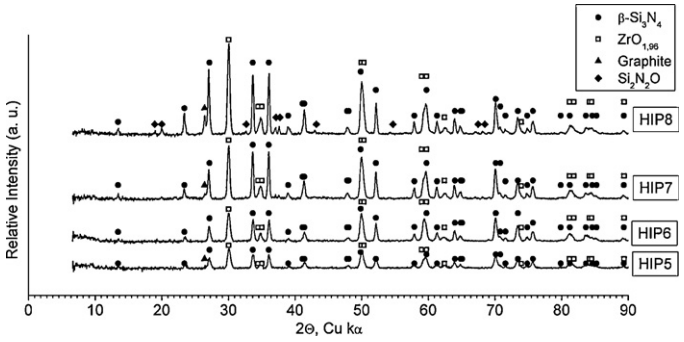

Fig. 6. XRD patterns of the sintered silicon nitride-based composites with 3 wt% graphene addition.

Table 2
Mechanical properties of the sintered graphene added silicon nitride composites.

Batch	Apparent density (g/cm^3)	Modulus of easticity (GPa)	4-point bending strength (MPa)
HIP1	3.379 ± 0.035	225.671 ± 6.220	506.243 ± 19.129
HIP2	3.375 ± 0.011	216.329 ± 5.977	420.057 ± 16.346
HIP3	3.367 ± 0.013	231.500 ± 2.882	535.943 ± 88.284
HIP4	3.328 ± 0.018	239.513 ± 6.844	642.763 ± 85.251
HIP5	3.031 ± 0.019	147.767 ± 4.650	308.167 ± 19.284
HIP6	3.063 ± 0.020	164.625 ± 30.127	319.025 ± 56.743
HIP7	3.024 ± 0.014	144.171 ± 14.523	326.143 ± 31.245
HIP8	3.319 ± 0.018	188.314 ± 4.680	451.829 ± 31.484

in Fig. 7. In the case of 1 wt% carbon content the elastic modulus showed increased values compared to the 3 wt%. In the case of MLG added silicon nitride composites (HIP4 and HIP8) enhanced values of the modulus can be seen. In particular in the case of the 3 wt% carbon content a relative increase of 14% in comparison to the second higher result (HIP6) could be observed.

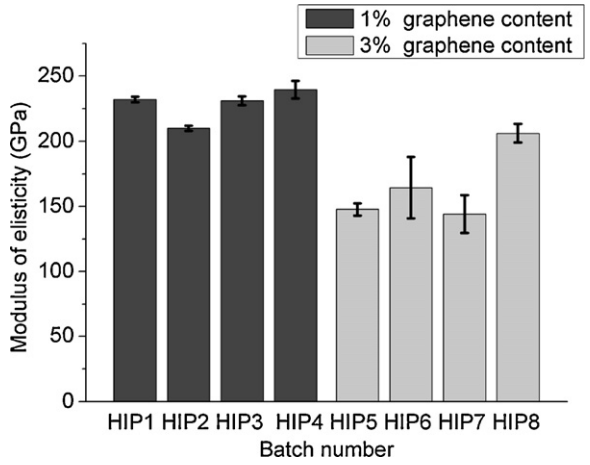

Fig. 7. Modulus of elasticity of the sintered ceramic composites with different type and quantity of graphene addition (HIP1 – HIP8).

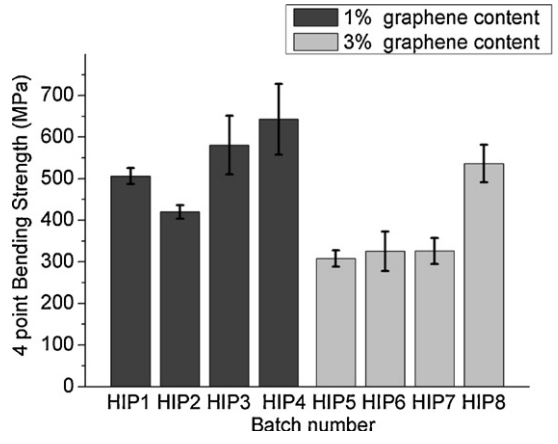

Fig. 8. Four point bending strength of the sintered ceramic composites with different type and quantity of graphene addition (HIP1 – HIP8).

The average results of the 4 point bending strength measurements are presented in Fig. 8. The same tendency to the observations related to the elasticity measurement have been observed. The superior mechanical properties of the MLG/silicon nitride composites (HIP4 and HIP8) can be observed. In the case of the 1 wt% graphene content an increase of 20% and – in the case of 3 wt% graphene content –, 38% can be measured in comparison to the second higher result (HIP3 and HIP7). These differences can be explained by not only the type and quality of the starting materials, but by the dispersion of graphene and by the differences of the apparent density of the samples. The samples with higher densities showed higher values respectively.

The decrease of the modulus of elasticity and the bending strength in the case of the samples with 3 wt% in comparison to 1 wt% carbon content can be noticed. This observation can be explained by the increase of the porosity formed around the graphite layers as shown previously by SEM micrographs. As a matter of fact only the mechanical properties of MLG added composite (HIP8) aproaches the modulus of elasticity and the bending strength values of the 1 wt% carbon added composites.

4. Conclusions

Silicon nitride based nanocomposites have been prepared with different ammount (1 and 3 wt%) of multilayer graphene (MLG) as well as exfoliated graphite nanoplatelets (xGnP) and nano graphene platelets (Angstron) in comparison. The microstructure and mechanical properties of the graphene reinforced ceramic composite materials have been investigated. Homogeneous distribution of the MLG additives on the fracture surface of the sintered specimens can be observed. SEM investigations showed that graphene sheets with approximately 10 nm in thickness may be observed embedded to silicon nitride matrix. The graphene platelets have been found to induce porosity in matrix. This may cause the deteriation of mechanical properties. It seems that the appropiate separation of the agglomerated graphene platelets in matrix has to be the key objective of the further works. Good connection between matrix and additions and decreasing the porosity should be achieved. In this work the key mechanical properties of graphene added silicon nitride-based ceramic composites have been also investigated. The bending strength and elastic

modulus of MLG/Si_3N_4 composites showed enhanced values compared to the other commercial graphene nanoplatelets added silicon nitride ceramic composites. These results can be explained by not only the type and quality of the starting materials, but by the dispersion grade of graphene having direct impact to resulting density of the sintered compacts. Further experiments are intended to explore the electrical, thermal and tribological behaviour of MLG/Si_3N_4 composites.

Acknowledgements

We would like to thank L. Illés and Z.E. Horváth for SEM and XRD measurements. We are grateful to preparation work of A. Petrik and V. Varga. We thank to P. Arató for helpful discussions.

References

[1] A.K. Geim, K.S. Novoselov:, The rise of graphene, Nat. Mater. 6 (2007) 183–191.
[2] M. Segal, Selling graphene by the ton, Nat. Nanotechnol. 4 (2009) 612–614.
[3] A.A. Balandin, S. Ghosh, W. Bao, I. Calizo, D. Teweldebrhan, F. Miao, C.N. Lau:, Superior thermal conductivity of single-layer graphene, Nano Lett. 8 (2008) 902–907.
[4] C.N.R. Rao, A.K. Sood, K.S. Subrahmanyam, A. Govindaraj:, Graphene: the new two-dimensional nanomaterial, Angew. Chem. Int. Ed. 48 (42) (2009) 7752–7777.
[5] C. Soldano, A. Mahmood, E. Dujardin:, Production, properties and potential of graphene, Carbon 48 (2010) 2127–2150.
[6] T. Ramanathan, A.A. Abdala, S. Stankovich, D.A. Dikin, M. Herrera-Alonso, R.D. Piner, D.H. Adamson, H.C. Schniepp, X. Chen, R.S. Ruoff, S.T. Nguyen, I.A. Aksay, R.K. Prud'Homme, L.C. Brinson:, Functionalized graphene sheets for polymer nanocomposites, Nat. Nanotechnol. 3 (2008) 327–331.
[7] Y. Fan, L. Wang, J. Lib, J. Lia, S. Sun, F. Chen, L. Chen, W. Jiang, Preparation and electrical properties of graphene nanosheet/Al_2O_3 composites, Carbon 48 (2010) 1743–1749.
[8] A. Peigney, Ch. Laurent, E. Flahaut, A. Rousset:, Carbon nanotubes in novel ceramic matrix nanocomposites, Ceram. Int. 26 (6) (2000) 667–683.
[9] R.Z. Ma, J. Wu, B.Q. Wei, J. Liang, D.H. Wu, Processing and properties of carbon nanotubes-nano-SiC ceramic, J. Mater. Sci. 33 (21) (1998) 5243–5246.
[10] C. Balázsi, B. Fényi, N. Hegman, Z. Kövér, F. Wéber, Z. Vértesy, Z. Kónya, I. Kiricsi, L.P. Biró, P. Arató:, Development of CNT/Si_3N_4 composites with improved mechanical and electrical properties, Composites: Part B 37 (2006) 418–424.
[11] S. Pasupuleti, R. Peddetti, S. Santhanam, K.P. Jen, N.Z. Wing, M. Hecht, P.J. Halloran, Mater. Sci. Eng. A491 (2008) 224–229.
[12] G.D. Zhan, J.D. Kuntz, J. Wan, A.K. Mukherjee, Nat. Mater. 61 (2) (2003) 38–42.
[13] Z. Xia, L. Riester, W.A. Curtin, H. Li, B.W. Sheldon, J. Liang, B. Chang, J.M. Xu, Acta Mater. 52 (2003) 931–944.
[14] G. Yamamoto, M. Omori, T. Hashida, H. Kimura, A novel structure for carbon nanotube reinforced alumina composites with improved mechanical properties, Nanotechnology 19 (2008) 1–7.
[15] I. Ahmad, A. Kennedy, Y.Q. Zhu, Carbon nanotubes toughened aluminium oxide nanocomposites, J. Eur. Ceram. Soc. 30 (2010) 865–873.
[16] X. Wang, N.P. Padture, H. Tanaka:, Contact-damage-resistant ceramic/single-wall carbon nanotubes and ceramic/graphite composites, Nat. Mater. 3 (2004) 539–544.
[17] J. Dusza, G. Blugan, J. Morgiel, J. Kuebler, F. Inam, T. Peijs, et al., Hot pressed and spark plasma sintered zirconia/carbon nanofiber composites, J. Eur. Ceram. Soc. 29 (15) (2009) 3177–3184.
[18] J. González-Julián, Y. Iglesias, A.C. Caballero, M. Belmonte, L. Garzon, C. Ocal, P. Miranzo, M.I. Osendi, Multi-scale electrical response of silicon nitride/multi-walled carbon nanotubes composites, Compos. Sci. Technol. 71 (1) (2011) 60–66.
[19] S. Yoshio, J. Tatami, T. Wakihara, T. Yamakawa, H. Nakano, K. Komeya, T. Meguro, Effect of CNT quantity and sintering temperature on electrical and mechanical properties of CNT-dispersed Si_3N_4 ceramics, J. Ceram. Soc. Jpn. 119 (2011) 70–75.
[20] J. Tatami, T. Katashima, K. Komeya, T. Meguro, T. Wakihara, J. Am. Ceram. Soc. 88 (2005) 2889–2893.
[21] E.L. Corral, H. Wang, J. Garay, Z. Munir, E.V. Barrera, Effect of single-walled carbon nanotubes on thermal and electrical properties of silicon nitride processed using spark plasma sintering, J. Eur. Ceram. Soc. 31 (3) (2011) 391–400.
[22] P. Hvizdoš, A. Duszová, V. Puchý, O. Tapasztó, P. Kun, Cs. Balázsi:, Wear behavior of ZrO_2-CNF and Si_3N_4-CNT nanocomposites, Key Eng. Mater. Vol. 465 (2011) 495–498.
[23] R. Poyato, A.L. Vasiliev, N.P. Padture, H. Tanaka, T. Nishimura, Nanotechnology 17 (2006) 1770–1777.
[24] E.L. Corral, L. Cesarano, A. Shyam, E. Lara-Curzio, N. Bell, J. Stuecker, N. Perry, M. Di Prima, Z. Munir, J. Garay, E.V. Barrera:, Engineered nanostructures for multifunctional single-walled carbon nanotube reinforced silicon nitride nanocomposites, J. Am. Ceram. Soc. 91 (2008) 3129–3137.
[25] P. Kun, F. Wéber, Cs. Balázsi, Preparation and examination of multilayer graphene nanosheets by exfoliation of graphite in high efficient attritor mill, Cent. Eur. J. Chem. Vol. 9 (1) (2011) 47–51.
[26] C. Knieke, A. Berger, M. Voigt, R.N. Klupp Taylor, J. Röhrl, W. Peukert:, Scalable production of graphene sheets by mechanical delamination, Carbon 48 (2010) 3196–3204.
[27] J. Lu, I. Do, H. Fukushima, I. Lee, L.T. Drzal:, Stable aqueous suspension and self-assembly of graphite nanoplatelets coated with various polyelectrolytes, J. Nanomater. 186486 (2010) 1–11, Article ID.
[28] http://www.xgsciences.com/.
[29] http://angstronmaterials.com.
[30] Cs. Balázsi, F.S. Cinar, O. Addemir, F. Wéber, P. Arató, Manufacture and examination of C/Si_3N_4 nanocomposites, J. Eur. Ceram. Soc. 24 (2004) 3287–3294.